Journal of Evolving Space Activities
Vol. 2, Article No. 167, 2024
DOI: 10.57350/jesa.167

# Development of the Fairing Structure for CALLISTO

By Silas EICHEL,[1)] Sofia GIAGKOZOGLOU VINCENZINO,[1)] and Markus MARKGRAF[2)]

[1)]*Institute of Structures and Design, DLR Stuttgart, Germany*
[2)]*Space Operations and Astronaut Training, DLR Oberpfaffenhofen, Germany*

(Received August 22nd, 2023)

In the frame of the project CALLISTO (Cooperative Action Leading to Launcher Innovation in Stage Toss back Operations), DLR, JAXA and CNES develop a demonstrator for a reusable, vertical take-off, vertical landing rocket first stage. The need for reusability of launchers imposes a new set of loads and requirements to almost every part of the rocket. Former flight heritage does not cover the descent and landing phase sufficiently. This lack of information is currently part of many investigations all around the space industry. CALLISTO aims to gather flight data and technological knowledge to achieve such return missions. This paper focuses on the development of the fairing and presents the design, major FE analysis results and performed test activities to achieve a lightweight and reusable space structure. As there is no payload deployed, the fairing is connected to the vehicle for the whole flight acting as a primary structure. Analyses show, that most of the driving loads are induced at the descent phase. In particular the thermal environment during this phase is dimensioning for the CFRP sandwich structure, which is equipped with a cork TPS.

**Key Words:** CALLISTO, Reusability, Structure, Test, Material

## Nomenclature

| | | |
|---|---|---|
| AoA | : | Angle of Attack |
| ALS | : | Approach and Landing System |
| CALLISTO | : | Cooperative Action Leading to Launcher Innovation for Stage Toss-back Operations |
| CDR | : | Critical Design Review |
| CFD | : | Computational Fluid Dynamics |
| CFRP | : | Carbon Fiber Reinforced Polymers |
| CMC | : | Ceramic Matrix Composite |
| CNES | : | Centre National d'Études Spatiales |
| CSG | : | Centre Spatial Guyanais |
| DLR | : | Deutsches Zentrum für Luft- und Raumfahrt e.V. |
| EM | : | Engineering Model |
| EQM | : | Engineering and Qualification Model |
| FCS/A | : | Flight Control System / Aerodynamic |
| FEM | : | Finite Element Model |
| FM | : | Flight Model |
| FNS | : | Flight Neutralization System |
| FS | : | Flight Spare |
| GNSS | : | Global Navigation Satellite System |
| JAXA | : | Japan Aerospace eXploration Agency |
| LH2 | : | Liquid Hydrogen |
| LLRM | : | Latch, Lock and Release Mechanism |
| LOX | : | Liquid OXygen |
| MRO | : | Maintenance and Repair Operations |
| NFM | : | Nose Fairing Module |
| PDR | : | Preliminary Design Review |
| RLV | : | Reusable Launch Vehicle |
| TGA | : | Thermogravimetric Analysis |
| TPS | : | Thermal Protection System |
| VEB | : | Vehicle Equipment Bay |

## 1. Introduction

Reusability in space launch systems is expected to increase their competitiveness and is therefore part of numerous investigations throughout the space industry. The advantage of reusable systems is a decrease of launch costs in a long-term perspective. Furthermore, reusability leads to more sustainability in space transportation. This analysis led to the start of the CALLISTO project in June 2017. The shared goal is to develop, build and fly a reusable scaled rocket stage taking-off and landing vertically.[1)] The CALLISTO vehicle is a flight demonstrator for future reusable launcher stages and their key technologies.[2)] The program involves three countries and their space organizations: CNES for France, DLR for Germany and JAXA for Japan. The flight campaign will be conducted in 2026/2027 in CSG, Europe's Spaceport. The know-how to be built includes products and vehicle design, ground segment set up, and post-flight operations for vehicle recovery and subsequent reuse.[3)] The breakdown of responsibilities between the three partners is depicted in Fig. 1.[4)]

The flight campaign is set up with up to ten flights in an incremental approach, systematically increasing the height, complexity and energy level of each flight. Minimal risk is also a main advantage of an incremental approach. The last two flights can be seen as demo flights to prove the capability to perform relevant flight envelopes for operational launch vehicles.[5)] CALLISTO aims to gather technical, economic and operational data to better evaluate if and under which boundary conditions Reusable Launch Vehicles (RLVs) are recommended. It also matures relevant technologies in that specific domain. Especially the gathering of flight data will improve and accelerate future launch vehicle developments.[6)]

CALLISTO's demo flight envelope, displayed in Fig. 2, is characterized by a classic ascent phase, a powered tilt-over and boost back maneuver, an aerodynamically controlled descent in the transonic region, and a landing phase to a dedicated landing zone.[7, 8] This flight envelope induces a whole new set of loads to almost all parts of the vehicle.

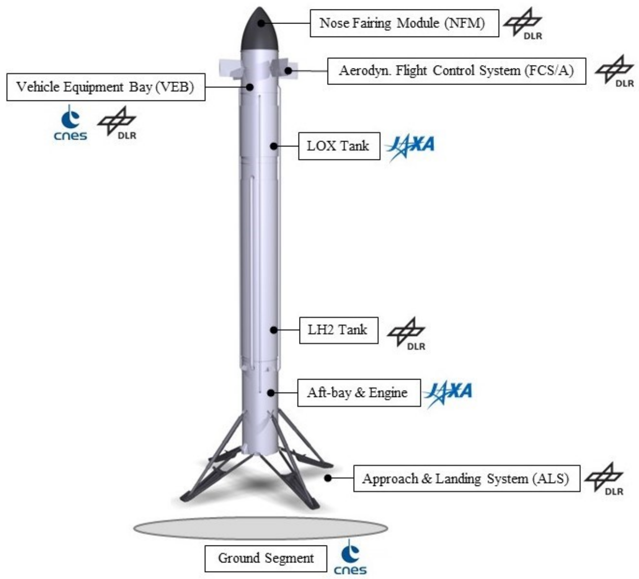


Fig. 1. The main structures and responsibilities of CALLISTO, a 13.5 m tall demonstrator rocket.[4)]

As there is no payload deployed, the fairing of CALLISTO is connected to the vehicle for the whole flight, acting as a primary structure. Thus, the fairing is exposed to the loads of the descent and landing phase as the rear of the vehicle, which enables the gathering of data in that particularly interesting flight phase.

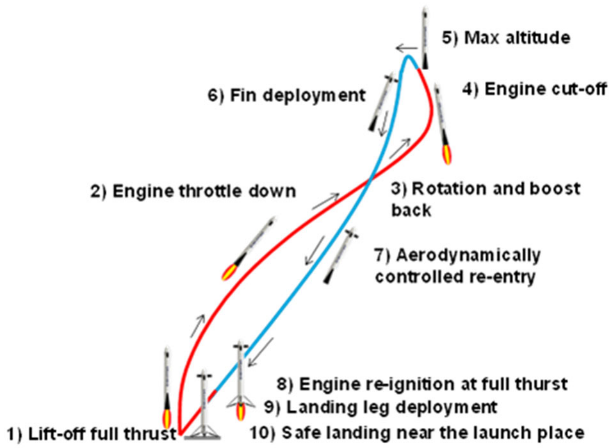


Fig. 2. Sketch of the demo flight path of CALLISTO.[8)]

The primary function of the Nose Fairing Module (NFM) is to protect the top of the CALLISTO demonstrator from aerodynamic flow. This is of particular necessity during the ascent flight phase. In addition, it accommodates the Global Navigation Satellite System (GNSS) antenna at the very top of the vehicle and parts of the Flight Neutralization System (FNS) on the inner wall.

This paper outlines the development activities for the fairing structure of CALLISTO. It presents the design description as well as the development approach and gives an update of the hardware status in the first part. Secondly, the flight load assessment is briefly introduced and the conducted FEM analyses on fairing side are presented with their major results. Then, already conducted and planned test activities are detailed. Afterwards, relevant MRO aspects are outlined before this paper concludes with an outlook to the future.

## 2. Baseline design

The fairing structure consists of three sub-assemblies, which are depicted in Fig. 3.:

1. Nose sub-assembly
2. Ogive main body
3. Aerocover

The nose sub-assembly (box no. 1) is located on the very top of the module to both accommodate the GNSS antenna and ensure best signal qualities. It is depicted in a section view in Fig. 4 with the GNSS antenna highlighted in yellow. The radome of the nose sub-assembly is made from a radio frequency transparent material. It is designed as a closed chamber to prevent condensation onto internal humidity-sensitive electrical components of the antenna. This is especially important for the descent phase, as the atmospheric pressure increase causes potentially humid air to enter into the inside compartments of the vehicle. The nose sub-assembly is equipped with two redundant one-way valves to reduce the pressure loads during the ascent. As the valves are closed during decent, the resulting under pressure has to be withstood by the structure. However, this is more favorable than to withstand overpressure during ascent. The whole sub-assembly can be taken off in a sealed state in order to open and evaluate the status of the antenna in a controlled environment in-between the flights.

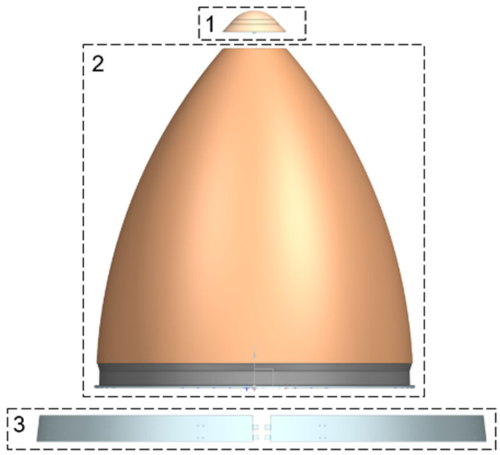


Fig. 3. The fairing separated into its three sub-assemblies.

The ogive main body (box no. 2) is the largest structure of the module. It is made from a CFRP sandwich with an aluminum L-flange bottom interface towards the vehicle equipment bay (VEB), an aluminum nose interface towards the nose sub-assembly, and a cork thermal protection system (TPS) on the outside. The CFRP sandwich is optimized for the thermomechanical loads driven by aerodynamic pressure on the outside and deformations due to aerodynamic forces onto the fins of the FCS/A. Therefore, not only the number of plies is locally decreased, but also the sandwich core is divided to implement a lighter core material on less stressed areas. The joints to the aluminum interfaces are glued with high-temperature epoxy adhesive due to severe thermally induced stresses. On the inside wall, parts of the FNS are attached by dedicated aluminum brackets.

An aerodynamic cover (box no. 3) is added in four segments to the bottom interface over the L-flange to reduce drag. This thin aluminum sheet metal is riveted to three brackets each segment. Its upper edge is in contact with the cork TPS, which is beneficial especially with respect to vibrations. The cork serves as a damper to the structure and prevents excess deformation.

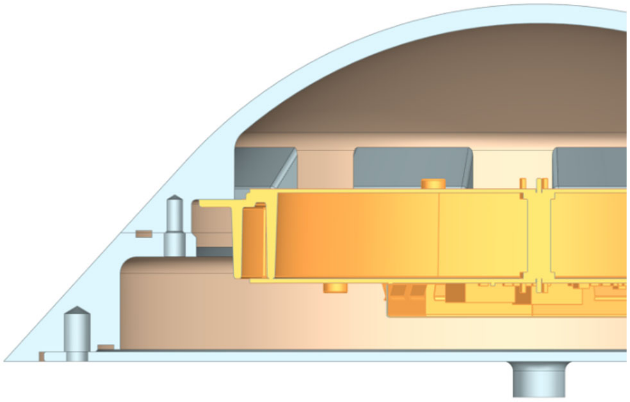

Fig. 4. The nose sub-assembly is designed as a sealed compartment. The GNSS Antenna is highlighted in yellow.

The outer surface will be covered with anti-static paint. Besides its electrical properties, it also improves the thermal coefficients for emissivity and absorptivity and reduces the temperatures of the structure and equipment.

### 2.1. Development approach

The main structures of the NFM will be developed in a prototype approach. In order to save resources, only one combined engineering and qualification model (EQM) will be built prior to the flight model (FM) and the flight spare (FS). The EQM serves to qualify both the design itself and also all the operations conducted during the flight campaign in CSG (French Guiana).

The Nose sub-assembly is developed with one engineering model (EM), two EQMs and several FMs. The use of two EQMs allows to speed up the qualification as one is used for mechanical aspects and the other is used for functional qualification of the GNSS system. The use of several flight models reduces the time to refurbish the fairing Module in between two flights. Each FM contains an identical GNSS antenna, which requires extensive checks after each flight, but due to additional hardware not necessarily before the next flight.

### 2.2. Hardware status

The EQM is almost completely assembled at the time of the submission, as shown in Fig. 5. The cork TPS is applied in segments onto the double curved surface of the CFRP sandwich. They were cut out from plain sheets in corresponding flat patterns. The gap between neighboring cork segments is less than 1 mm for most cases. The effect of the residual gap is currently under investigation.

Fig. 5. The fairing EQM is currently assembled.

In the next steps, the anti-static paint of white color as well as the FNS and corresponding instrumentation will be integrated prior to module qualification testing.

## 4. Flight Load Assessment

The fairing is subjected to several sets of combined loads of thermal, mechanical and vibrational manner. Extensive analysis took place by all three partners to master the assessment of induced flight loads.

On DLR side, the load assessment was conducted with focus on the aerothermal environment. Detailed CFD analyses led to a database, from which specific load requirements were derived for each module the vehicle consists of. Example parameters of interest include vehicle flight orientation, angle of attack (AoA), velocity, altitude, and vehicle configuration. Details on the flight load assessment process and corresponding analysis details are shown in 9), 10) and 4).

One major result of this work is a thermal environment requirement definition in five zones as shown in Fig. 6.

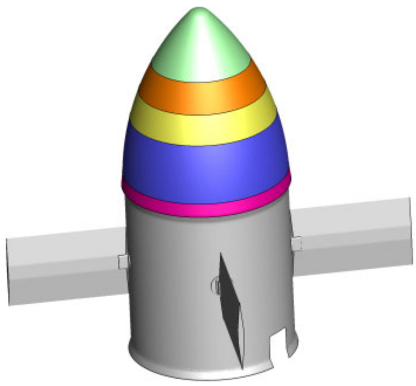

Fig. 6. The thermal requirement is defined in five zones. The remaining part of the top block is displayed for orientation.

The mechanical loads also play a key role for the structural design. They are driven by two main contributors:

- Aerodynamic pressure distributions on the outer surface.
- Deformations imposed to the whole top block by fin deflections.

The combination of both loading types results in a total set of 28 load cases, for which 2 correspond to the ascent phase of the vehicle trajectory and 26 to the descent phase. This calculation illustrates the enormous effort needed to master the vehicle descent.

## 5. Thermomechanical Analysis

The structural analysis was conducted with a combined model of the fairing and the VEB, as the load cases are dependent on the total deformation of both products. The fin deflections are implemented at the fin-VEB interface via dedicated forces and moments. The fins themselves are therefore not part of the fairing simulations. The deformations of the fairing (and VEB) are visualized in Fig. 7. On the left side, the deformation of the fairing during a load case from the ascending part of the trajectory is visualized. On the right side, a load case from the descending part of the trajectory is presented.

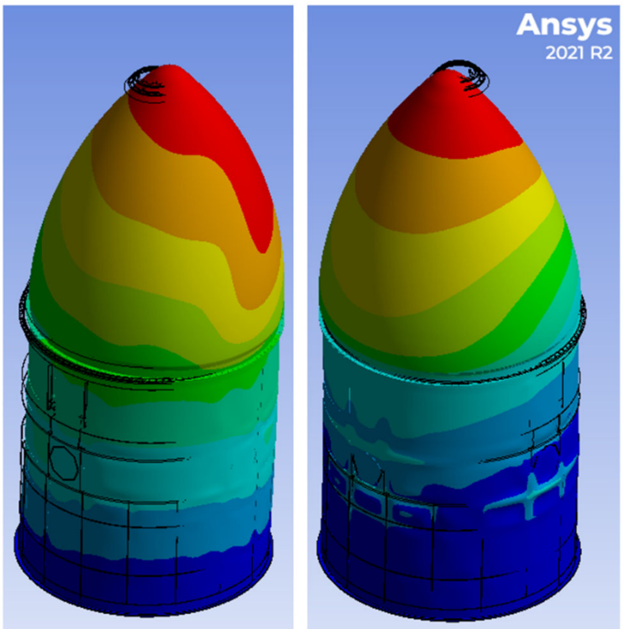


Fig. 7. Exemplary fairing (and VEB) deformation during the flight for 2 load cases obtained with Ansys. To increase the visibility, the real deformation is increased in both pictures. The left side shows an ascending load case, the right side a descending load case. Red marks maximum displacement and blue minimum displacement.

The analyses were conducted with special attention to load cases, where increased temperatures are present as this affects the mechanical properties of the used materials. This is especially critical for combinations of materials with huge differences in the thermal expansion coefficients. For the fairing, the most critical combination is aluminum and CFRP. At the very last flight phase, hot exhaust gas from the engine forms a plume around the vehicle and heats the aluminum structure at the bottom to ~101 °C. Figure 8 shows the temperature distribution of the bottom interface at that time of the flight, representing the dimensioning load case for the junction of the aluminum L-Flange and the CFRP sandwich. This scenario also implies that a high-temperature adhesive is necessary.

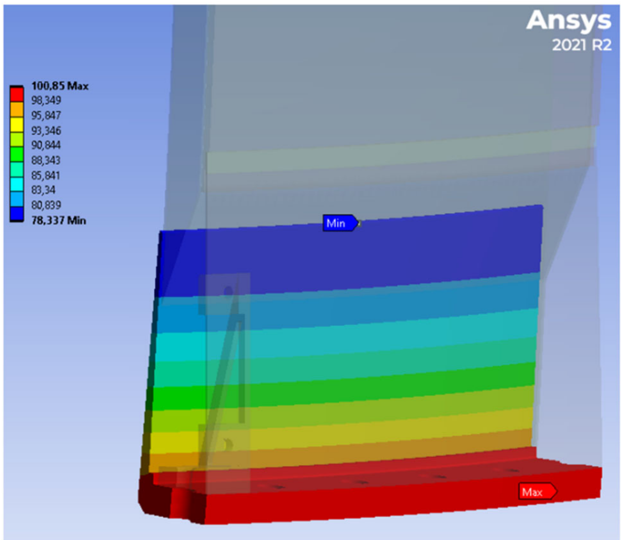


Fig. 8. Temperature distribution of a section of the fairing bottom interface in [°C] at peak temperatures obtained with Ansys.

Dedicated analyses were conducted to predict the temperature of the fairing for not only the flight, but also the pre- and post-flight phases, which could last for several hours. The prior formulation of dedicated zones as displayed in Fig. 6 allows for a separation of the fairing into smaller sub-models, which drastically decreases the simulation time. One major result of the analyses is the need for a TPS on the outside of the CFRP, as no suitable CFRP resin is able to withstand both temperatures and mechanical loads at the end of the flight of CALLISTO.

Based on these considerations, the fairing TPS is made of cork. It is a suitable material commonly used as an ablative heatshield, especially for return missions[11)]. However, in the case of the CALLISTO fairing, it is used as a non-ablative isolator. The temperatures on the outside of the cork reach ~220 °C. Thermogravimetric analyses (TGA) show a density change at that temperature[12)], which indicates that the ablative process of pyrolysis may already take place. However, as the exposure time is very limited, the chemical reactions during pyrolysis may not even start. The corresponding TGA[12)] was conducted as state of the art at very slow heating rates, which is contrary to what is happening during the flight of CALLISTO. As this temperature is just crossing the temperatures of pyrolysis process, cork as a non-ablative TPS is a concept which needed confirmation by tests and is detailed in chapter 6. It was shown there, that no pyrolysis is taking place under that specific thermal environment, which makes cork a suitable isolator for reusable missions in that temperature regime. That also means that no major MRO activity concerning the fairing TPS is needed between two flights.

In case of an unplanned event or excessive loads which might result in a higher temperature, any changes on the cork TPS can be easily identified during visual inspections. Pyrolysis would be recognizable by a dark or even black burned color. In such a case, the pyrolysis would absorb the additional heat and protect the CFRP structure. In subsequent corrective maintenance operations, the cork in those regions will be replaced.

Focusing on the top of the fairing, the nose sub-assembly contains the humidity-sensitive GNSS antenna. Therefore, the nose sub-assembly is designed as a closed chamber. It features two one-way valves, which will let air out of this section but not back inside. The GNSS antenna will be installed and sealed in a controlled environment and purged with dry air. During the ascent, air will flow from the inside of the nose sub-assembly into the inner main volume of the fairing. In contrast, the valves block the potentially humid air to enter the compartment with the GNSS antenna during descent. This also means that a pressure difference is present. Due to the valves, this will be an internal under pressure only. This is favorable from a mechanical point of view, as potential cracks in the structure are pressed together and will therefore not evolve as quickly until potential failure of the structure, when compared to tension due to over pressure.

## 6. Test Activities

During the course of the development, several smaller subsystem tests were conducted in order to either justify the analytical design or qualify specific parts for the use within CALLISTO. This chapter outlines the tests already completed and presents an outlook to the main qualification campaign.

### 6.1. Cork heat tests

As outlined in chapter 5, the use of cork as a non-ablative TPS for the fairing of CALLISTO needs additional justification through dedicated tests.

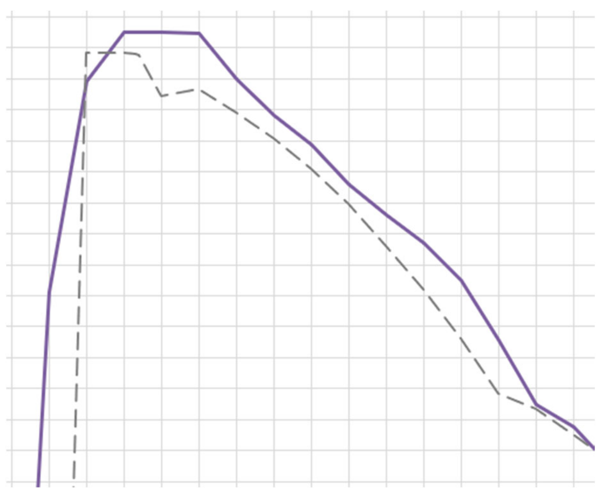

Fig. 9. Temperature over time of the cork heat test. In dashed line: Expected temperature of the gas in flight. Continuous line: Temperature of the gas as measured during the test. The graph is horizontally divided for every 10 °C and vertically divided for each second.

Therefore, samples of cork were prepared and subjected to a similar thermal environment as specified for the demo flight. A stream of hot air was directed onto the surface of the cork with a thermocouple directly in front of it. The measured temperature was used to compare the test temperature with the expected gas temperature during flight. By varying the distance to the nozzle of the hot air generator, the flight temperature profile was reproduced. The test temperature is shown in Fig. 9. As the temperature of the gas in the flight (dashed line) is almost always lower than the gas temperature in the test (continuous line), the test setting can be described as slightly conservative.

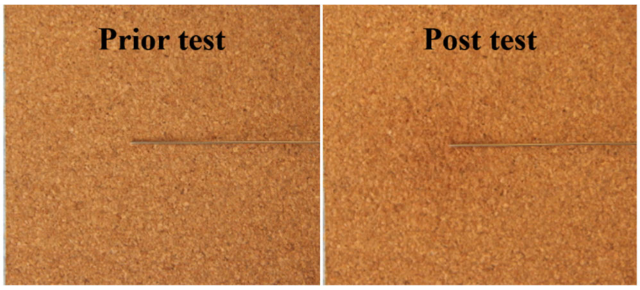


Fig. 10. Result of the cork samples of the heat tests (with thermocouple in front). No significant difference can be seen from prior to post test.

The result of the cork heat test is shown in Fig. 10. There is no burnt spot visible on the surface of the cork. This shows, that the cork is not or at least almost not affected by the temperature regime of the test. Hence, the concept of cork as a non-ablative TPS for CALLISTO is deemed suitable.

### 6.2. Equipment shaker tests

Severe vibration loads are expected for the equipment of CALLISTO. Therefore, dedicated shaker tests on equipment level were conducted to ensure functionality during flight. The GNSS antenna and the FNS attachments were tested in random and sinus vibration tests.

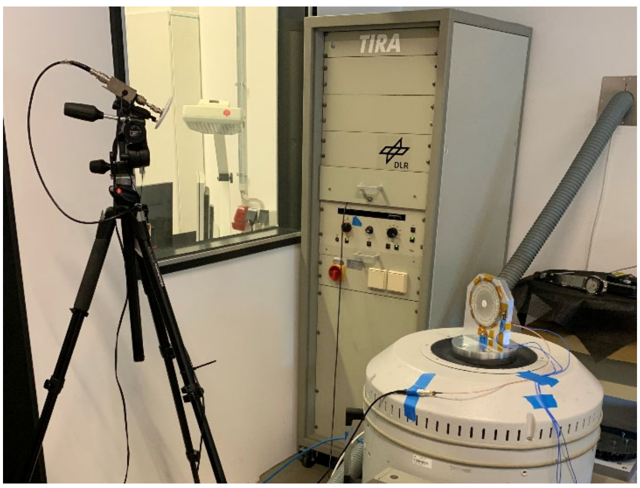


Fig. 11. CALLISTO GNSS antenna element mounted on top of the shaker with a 90°-adapter (right side) and re-radiation antenna installed on a tripod (left side) providing the device under test with artificial GNSS signal generated by a GNSS simulator.

The functionality of the GNSS antenna is crucial to the navigation system of CALLISTO and its proper functionality must be guaranteed in all flight phases. The GNSS antenna was connected to a GNSS navigation receiver during the test. Moreover, artificial GNSS signals were fed into the system via a signal re-radiation kit placed above the shaker table, as shown in 20. This specific hardware-in-the loop configuration allowed to continuously monitor and check the functionality and performance of the device under tests during the individual test runs. During none of the performed test runs neither a device failure nor any performance degradation has been observed.

The FNS attachments need to maintain their clamping functionality throughout the whole campaign. The tests were successfully completed over the whole life time of CALLISTO with no sign of weakening in the structure or the adhesive.

### 6.3. GNSS antenna radome characterization

In addition to the shaker tests described above, an initial series of antenna characterization tests were performed using a mock-up of the nose sub-assembly. This was necessary to assess the impact of the antenna radome, which is much thicker than recommended by the antenna manufacturer for stability and thermal reasons. Furthermore, the effect of the anti-static paint onto the receiving performance of the GNSS antenna element was quantified. The tests were conducted in an open-sky setup on the roof top of the DLR GSOC main building in two steps. In the first step, GNSS signal levels received with the unpainted mock-up were compared with values obtained with a well-characterized geodetic-grade reference antenna to determine the gain-loss caused by the radome material. The test was then repeated with the anti-static paint applied to the radome.

Fig. 12. Nose sub-assembly mock-up during the roof-top test performed to assess the impact of the anti-static paint onto the receiving performance of the GNSS antenna element.

While the first test revealed an additional attenuation of the received GNSS signal of 1 to 3 dB, depending on the GNSS frequency, constellation and elevation angle of the incoming signal, no effect was observed due to the anti-static paint. The observed overall attenuations are within the expected range and do not significantly degrade the achievable navigation accuracy and robustness of the PVT solution and are therefore acceptable.

Once a qualification model of the nose sub-assembly is available, another, more detailed, characterization campaign with the antenna will be conducted in the antenna laboratory of the DLR institute of communication and navigation. During this campaign, not only the receiving gain pattern of the antenna will be measured, but also the phase center location and the phase center variation. These values are important to reach a centimeter-level accuracy in the final landing phase.

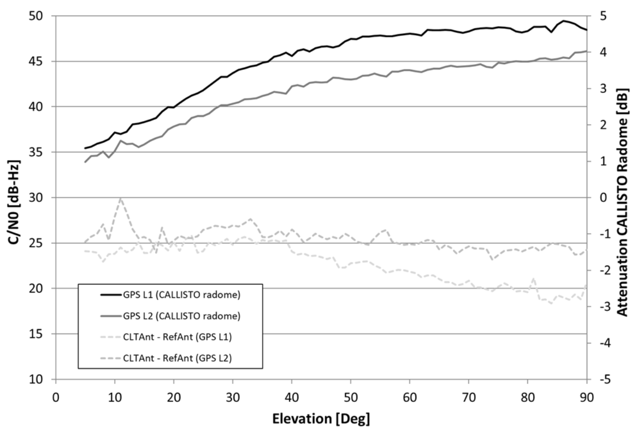


Fig. 13. Signal levels vs. elevation angle of incoming signal (solid lines) and measured additional attenuation of the CALLISTO radome compared to a reference antenna (dashed lines) for the GPS L1 and L2 frequencies.

### 6.4. Upcoming module tests

The qualification campaign will start after EQM assembly, which has been almost completed at the time of the submission. The fairing module will be subjected to thermal, static mechanical, vibrational and acoustic tests.

It is impossible to reproduce the transient thermal cycle of the flight in a laboratory. The focus is therefore put on the most critical aspects including the cork TPS and the thermal expansion of the aluminum bottom interface. As the cork has been already covered and validated by test, the module tests will concentrate on the thermal expansion of the bottom interface. Critical stress is induced by the fact that the CFRP structure on the outside has a significantly lower thermal expansion coefficient than the aluminum flange structure on the inside. Furthermore, this flange will not a have uniform temperature but a gradient with its maximum on the lower outer edge and its minimum on the upper inner edge, as shown in Fig. 8. To approach this gradient, the test will be conducted on a heating table. Before the fairing is placed on the table, it will be heated up to ~101 °C which equals the maximum temperature of the aluminum structure during the flight. Once the thick table top is completely heated to this temperature, the fairing will be placed onto the table. As soon as it is in contact with it, the heat is conducted into the structure with the bottom of the aluminum flange presumably heating up faster than the upper edge. The fairing is then lifted from the heating table as soon as the upper edge reaches its target temperature of ~79 °C. After that, the flange is expected to converge to a temperature somewhere in the middle. After ambient cooling, the structure will be inspected for defects in the aluminum, CFRP or adhesive layer in-between.

Mechanical structure tests are planned together with the VEB, as this represents the real boundary condition during flight. As the 3-dimensional pressure distribution on the outside is impossible to reproduce, the fairing will be subjected only to loading sourced by the fin deflections. It is therefore not a test to demonstrate robustness against structural failure. Its goal is rather to validate the FEM and show that the models are accurate enough to predict the behavior of the structure under loading. The test will be conducted with the fairing attached to the VEB and with fin dummy structures integrated to the VEB. Forces and moments according to the load cases from the design process are applied onto those dummy structures. The resulting deformation is measured and compared to the previously conducted FEM-analysis.

In dedicated vibrational tests, the fairing module will be subjected to sinus vibrations. The major goal of this test consists in the identification of the modes and damping properties of the whole module. This test is conducted without the VEB. As previously described in this section, random vibration tests were already conducted for the equipment GNSS antenna and FNS attachments.

Acoustic tests will be conducted on top block level which corresponds to the combination of fairing, VEB, and FCS/A. The tests will take place in Toulouse under the authority of CNES. This test serves to verify that the fairing structure dampens the vibrations in such a way that the equipment does not experience more vibrations than what was tested in the dedicated random shaker tests. Furthermore, it also verifies the structural integrity of the module. Especially thin structures, such as, for example, the aerocover shield are prone to acoustic loads.

In addition to these module tests, a nose sub-assembly pressure test is planned to verify that the structural integrity is given throughout the pressure differences during the flight as described in chapter 5.

## 7. MRO Aspects

Multiple-flight vehicles demand for fast refurbishment in order to be as efficient in service as possible. At the same time, MROs need to ensure a reliable detection of anomalies or defects and quick mitigation possibilities in case of off-nominal events. As an example, defects of the cork TPS due to off-nominal temperatures will be identified by visual inspection of the outer surface, as this area will turn dark during flight under increased temperatures. The fast and easy handling of the flight hardware is therefore of special importance and ensures an uncomplicated and safe detection process.

The fairing of CALLISTO is therefore put in a dedicated MRO frame, which allows easy access to every part of it. The frame and the fairing itself are shown in Fig. 14 in two different orientations. The frame consists of a hexagonal structure, which is attached to the fairing bottom interface. The hexagonal frame component can be rotated in the outer frame and locked in various orientations. The rotation axis is close to the center of mass, which allows the turning of the fairing by only one operator. After final qualification, the EQM will be used to quantify the duration of several planned and unplanned operations needed in CSG. The replacement of various parts, as, for example, parts of the cork TPS, instrumentation or FNS attachments can be trained on the EQM in realistic conditions.

Fig. 14. Fairing inside the MRO frame for assembly and MRO operations.

## 8. Conclusion

The fairing structure as a primary structure for the CALLISTO vehicle is subjected to key requirements for RLVs. Its development is well advanced and about to enter the final module qualification phase. All assessed environmental loads are identified and mastered within the current design. A number of specific critical aspects are already verified by subsystem tests. In addition, auxiliary tools for safe and fast refurbishment between two flights have been built and are ready to use. The planned module qualification will verify a thoroughly suitable design against all expected flight loads. Recorded data gathered during the upcoming flight campaign will significantly contribute to improve future RLV structure development in addition to the already assessed learnings during the design phase.

## Acknowledgments

The authors would like to thank the entire CALLISTO project team at CNES, JAXA, and DLR for their remarkable efforts and collaboration over the past years.

## References

1) Ishimoto, S., Tatiossian, P. and Dumont, E.: Overview of the CALLISTO Project, 32nd International Symposium on Space Technology and Science, Fukui, Japan, 2019-o-1-05, 2019, https://elib.dlr.de/132886/.
2) Dumont, E., Ishimoto, S., Tatiossian, P., Klevanski, J., Reiman, B. Ecker, T., Witte, L., Riehmer, J., Sagliano, M., Giagkozoglou Vincenzino, S., Petkov, I., Rotärmel, W., Schwarz, R., Seelbinder, D., Markgraf, M., Sommer, J., Pfau, D. and Martens, H.: CALLISTO: A Demonstrator for Reusable Launcher Key Technologies, *Trans. JSASS Aerospace Tech. Japan.* **19**, 1 (2021), pp. 106-115, https://doi.org/10.2322/tastj.19.106.
3) Dumont, E., Ishimoto S., Illig M., Sagliano M., Solari M., Ecker T. et al.: CALLISTO: towards reusability of a rocket stage: current status, 33rd International Symposium on Space Technology and Science, Oita, Japan, 2022, https://doi.org/10.57350/jesa.75.
4) Giagkozoglou Vincenzino, S., Eichel, S., Rotärmel, W., Krziwanie, F., Petkov, I., Dumont, E., Schneider, A., Schröder, S., Windelberg,

J., Ecker, T., and Ertl, M.: Development of Reusable Structures and Mechanisms for CALLISTO, 33rd International Symposium on Space Technology and Science, Oita, Japan, 2022, https://doi.org/10.57350/jesa.36.

5) Desmariaux, J., Cliquet Moreno, E., Chavagnac, C., Tatiossian, P. Saito, Y. and Dumont, E.: CALLISTO Reusable Vehicle System Design, 32nd International Symposium on Space Technology and Science, Fukui, Japan, 2019-g-02, 2019, https://elib.dlr.de/132889/.

6) Krummen, S., Desmariaux, J., Yasuhiro, S., Boldt, M., Briese, L., Cesco, N. Chavagnac, C., Cliquet Moreno, E., Dumont, E., Ecker, T., Eichel, S., Ertl, M., Giagkozoglou Vincenzino, S., Glaser, T., Grimm, C., Illig, M., Ishimoto, S., Klevanski, J., Lidon, N., Mierheim, O., Niccolai, J., Reershemius, S., Reimann, B., Riehmer, J., Sagliano, M., Scheufler, H., Schneider, A., Schröder, S., Schwarz, R., Seelbinder, D., Stief, M., Windelberg, J. and Woicke, S.: Towards a Reusable First Stage Demonstrator: CALLISTO - Technical Progresses & Challenges, 72nd International Astronautical Congress (IAC), Dubai, United Arab Emirates, IAC-21-D2.6.1, 2021, https://elib.dlr.de/147143/.

7) Guédron, S., Ishimoto, S., Dumont, E., Tatiossian, P., Chavagnac, C., Desmariaux, J., Monchaux, D., Frenoy, O., Cliquet Moreno, E., Deremaux, C., Lidon, N., Cesco, N., Witte, L., Sagliano, M., Seelbinder, D., Klevanski, J., Ecker, T., Reimann, B., Riehmer, J., Ertl, M., and Krummen, S.: CALLISTO DEMONSTRATOR: Focus on system aspects, 71st International Astronautical Congress (IAC), online, 2020, https://elib.dlr.de/138808/

8) Dumont, E., Sagliano, M., Eichel, S., Markgraf, M., Glaser, T., Braun, B., Windelberg, J., Petkov, I., Schröder, S., Witte, L., Schneider, A., Panthen, B., Häseker, J., Opp, L., Krieger, A., Stief, M., Woicke, S., Martens, H., Krummen, S.: CALLISTO: Reusable rocket stage demonstrator: getting ready for implementation, 34th International Symposium on Space Technology and Science (ISTS), Kurume in Fukuoka, Japan, 2023, https://elib.dlr.de/197208/

9) Ecker, T., Ertl, M., Klevanski, J., Krummen, S., and und Dumont, E.: Aerothermal characterization of the CALLISTO vehicle during descent, 9th European Conference for Aeronautics and Space Science (EUCASS), Lille, France, 2022, https://doi.org/10.13009/EUCASS2022-4680.

10) Schwamborn, D., Gerhold, T. and Heinrich, R.: The DLR TAU-code: Recent applications in research and industry. European Conference on Computational Fluid Dynamics (ECCOMAS CFD), Egmond aan Zee, The Netherlands, 2006.

11) Drescher, O., Hörschgen-Eggers, M., Pinaud, G., and Podeur, M.: Cork based thermal protection system for sounding rocket applications – development and flight testing, 23rd ESA PAC Symposium, Visby, Schweden, 2017, https://elib.dlr.de/116387/

12) Böhrk, H., and Stokes, J.: Kinetic Parameters and Thermal Properties of a Cork-Based Material, 20th AIAA International Space Planes and Hypersonic Systems and Technologies Conference, Glasgow, UK, 2015, https://doi.org/10.2514/6.2015-3532